aerospace

Article

A Novel Efficient Prediction Method for Microscopic Stresses of Periodic Beam-like Structures

Yufeng Xing [1], Lingyu Meng [1,2], Zhiwei Huang [1] and Yahe Gao [1,*]

[1] School of Aeronautic Science and Engineering, Beihang University, Beijing 100191, China
[2] Shen Yuan Honors College, Beihang University, Beijing 100191, China
* Correspondence: gaoyahe@buaa.edu.cn

Abstract: This paper presents a novel superposition method for effectively predicting the microscopic stresses of heterogeneous periodic beam-like structures. The efficiency is attributed to using the microscopic stresses of the unit cell problem under six generalized strain states to construct the structural microscopic stresses. The six generalized strain states include one unit tension strain, two unit bending strains, one unit torsion strain, and two linear curvature strains of a Timoshenko beam. The six microscopic stress solutions of the unit cell problem under these six strain states have previously been used for the homogenization of composite beams to equivalent Timoshenko beams (Acta. Mech. Sin. 2022, 38, 421520), and they are employed in this work. In the first step of achieving structural stresses, two stress solutions concerning linear curvatures are transformed into two stress solutions concerning unit shear strains by linearly combining the stresses under two unit bending strains. Then, the six stress solutions corresponding to six generalized unit beam strains are combined together to predict the structural microscopic stresses, in which the six stress solutions serve as basic stresses. The last step is to determine the coefficients of these six basic stress solutions by the principle of the internal work equivalence. It is found that the six coefficients, in terms of the product of the inverse of the effective stiffness matrix and the macroscopic internal force column vector, are the actual generalized strains of the equivalent beam under real loads. The obtained coefficients are physically reasonable because the basic stress solutions are produced by the generalized unit strains. Several numerical examples show that the present method, combining the solutions of the microscopic unit cell problem with the solutions of the macroscopic equivalent beam problem, can accurately and effectively predict the microscopic stresses of whole composite beams. The present method is applicable to composite beams with arbitrary periodic microstructures and load conditions.

Keywords: beam; asymptotic homogenization; periodic; Timoshenko; stress

Citation: Xing, Y.; Meng, L.; Huang, Z.; Gao, Y. A Novel Efficient Prediction Method for Microscopic Stresses of Periodic Beam-like Structures. *Aerospace* **2022**, *9*, 553. https://doi.org/10.3390/aerospace9100553

Academic Editor: Konstantinos Tserpes

Received: 6 August 2022
Accepted: 23 September 2022
Published: 26 September 2022

1. Introduction

Composite beam-like structures are widely used in engineering because of their excellent properties, such as high specific strength, high specific modulus, and corrosion resistance. The structure formed by the same unit cells lining up in one direction is called periodic beam structure. With the development of composite materials, these structures have become more complex than before in terms of material distributions and geometric configurations, leading to heavy computational loads in finite element analysis. To reduce the computational burden, many works have focused on homogenization methods to transform the original highly heterogeneous problem into a homogeneous problem. In addition to the homogenized or macroscopic solutions, some local or microscopic fields, e.g., microscopic stresses, are also of concern for failure analysis. Therefore, how to obtain the microscopic fields of composite beam-like structures based on homogenized solutions becomes a key problem.

To ensure the accurate construction of microscopic structural fields, obtaining a reasonable homogeneous structure is the important premise. The Asymptotic Homogenization

Method (AHM) [1,2], with a strict mathematical theory, has been proved to be very representative among various homogenization methods, and it can effectively predict the equivalent material properties of three-dimensional (3D) composite structures with omnidirectional periodicity. For periodic beam-like structures, the fewer unit cells in the thickness and width directions make the omnidirectional periodicity generally not hold, and thus the direct use of the AHM to beam structures may lead to unsatisfied accuracy; refer to the studies on cell size effects [3–5]. Different from the idea of material homogenization, Kolpakov [6–8] further extended the AHM to composite beam-like structures with periodicity only in the axial direction and obtained the equivalent Euler–Bernoulli beam models with effective sectional stiffnesses. The analytical solutions to unit cell problems, however, were difficult to achieve due to the complex periodic microstructures, and then a novel numerical implementation method [5] was proposed for the generalization of Kolpakov's method [6–8].

There are many other methods for the homogenization of sectional stiffnesses of composite beams. The variational asymptotic beam section analysis (VABS) [9–16], based on the variational idea, is one of the most powerful methods. In the VABS, different order models with or without the inclusion of shear effects were established to the desired equivalent Euler–Bernoulli or Timoshenko beam models. Huang et al. [17] starting directly with the fourth-order ordinary differential equations (for the Euler–Bernoulli problem) with periodic coefficients and proposed a two-scale asymptotic expansion method for periodic composite beams. In Huang et al.'s method [17], the deflections were asymptotically expanded and have been proved to be convergent via the two-scale convergence method [18,19]. For the achievement of equivalent Timoshenko beam models, shear stiffnesses have been taken into consideration in works [20–22], based on the strain energy equivalence of unit cells at macro- and microscales. These three methods [20–22] mainly differed in three aspects, including the different displacement forms used in microscopic fields, the different generalized beam strain states used for shear stiffness predictions, and the different boundary conditions used for solving unit cell problems. These methods [20–22] have their advantages. For instance, Huang et al.'s method [21] with two unit shear strain states has more clear physical meanings because the corresponding shear strain energies or shear forces are the desired effective shear stiffnesses, and this method is also more efficient because one can obtain six internal forces, i.e., six effective stiffnesses at a time. Compared with Huang et al.'s method [21], the other two methods [20,22] with the use of two linear curvature states are more accurate because constant shear forces always occur with linear bending moments.

How to obtain the 3D local or microscopic fields of composite beam-like structures has become a matter of concern after homogenization. With the homogenized sectional stiffnesses acquired in the VABS, the original heterogeneous 3D problem can be decomposed into a two-dimensional (2D) cross-sectional problem and a one-dimensional (1D) homogeneous beam problem. The 3D displacements, strains, and stresses over the cross section were then accurately recovered by the relations with the 1D macroscopic quantities [14,15,23–25]. Further, a variational asymptotic dimensional reduction model was developed for local recovery in fiber-reinforced polymer laminated beams [26]. Liu et al. [27] proposed a novel approach based on the mechanics of structure genomes for the homogenization (achievement of effective sectional stiffnesses) and dehomogenization (recovery of local fields) analyses of composite beam-like structures. Kashefi et al. [28] reproduced the 3D local fields for box girder bridge decks based on Giavotto's beam theory [29]. Dhadwal et al. [30] proposed a multifield variational formulation for the accurate recovery of local stress of multilayered beams. Xu et al. [31,32] successively developed solutions to Saint–Venant and Almansi–Michell problems of periodic composite beams, and the local stress components under different load cases were accurately captured, except for several unsatisfactory results near structural boundaries. Treyssede et al. [33] presented a two-dimensional formulation for predicting both macroscopic stiffness and microscopic stresses of helical beam-like structures. Hu et al. [34] recently developed a geometrically nonlinear refined beam model with the capability of capturing the coupling deformation effects and the local deformations near the force point. In addition, Sirimontree et al. [35] recently studied the structural behaviors of sandwich magneto-electro-elastic cylindrical nanoshells using the third-order shear deformation assumption, and their research on the influences of different parameters is of significance for practical application.

The feasibility and validity of the homogenization method recently proposed by Gao et al. [22] have been verified for periodic beam-like structures. However, the dehomogenization analysis for 3D local fields of structures has not been conducted and deserves research. The main contribution of this paper is to present a novel superposition method for effectively predicting the microscopic stresses of 3D periodic beams based on the homogenization method [22]. The novelty of the present superposition method lies in taking six kinds of microscopic stress solutions of the unit cell problem as the basic stresses and using the principle of two-scale internal work equivalence to determine the superposition coefficients. This equivalence principle ensures the accuracy of the present work.

The other parts of this paper are structured as follows: the process of the used effective stiffness prediction method is reviewed in Section 2, then the formulae for solving the micro-stresses are established in Section 3, and numerical examples are taken into account to show the validity of the present method in Section 4; finally, Section 5 gives the conclusions of this work.

2. The Homogenization Method for Periodic Timoshenko Beams

This section briefly reviews the homogenization (or effective stiffness prediction) method [22] proposed for periodic beam-like structures. In this method, a heterogeneous 3D structure can be treated as a homogeneous Timoshenko beam with equivalent stiffnesses, see the sketch of the homogenization process in Figure 1.

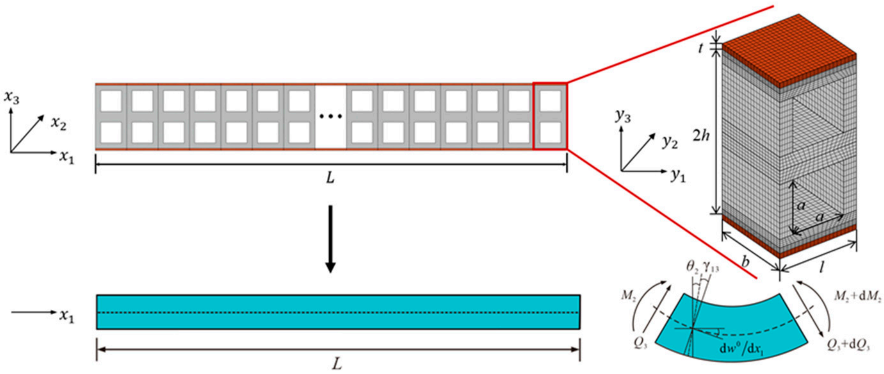

Figure 1. Sketch of homogenization process.

The generalized constitutive relationship of a homogenized Timoshenko beam is defined as:

$$\boldsymbol{F} = \boldsymbol{D}\boldsymbol{\varepsilon}_{1\mathrm{D}} \rightarrow \begin{bmatrix} N_1 \\ M_3 \\ M_2 \\ T_1 \\ Q_2 \\ Q_3 \end{bmatrix} = \begin{bmatrix} D_{11} & & & & & \\ & D_{22} & & & & \\ & & D_{33} & & & \\ & & & D_{44} & D_{45} & D_{46} \\ & & & D_{54} & D_{55} & \\ & & & D_{64} & & D_{66} \end{bmatrix} \begin{bmatrix} \varepsilon_1 \\ \kappa_3 \\ \kappa_2 \\ \kappa_1 \\ \gamma_{12} \\ \gamma_{13} \end{bmatrix} \tag{1}$$

where $\boldsymbol{F}$ and $\boldsymbol{\varepsilon}_{1\mathrm{D}}$ respectively denote the generalized internal forces and beam strains. Note that, in this work, only the most common tension-bending (D_{12}, D_{13}) and shearing-torsion (D_{45}, D_{46}) coupling stiffnesses are considered besides the diagonal stiffnesses $D_{\alpha\alpha}$ (α = 1, 2, 3, 4, 5, 6), and the tension-bending coupling terms (D_{12}, D_{13}) can be eliminated by setting the coordinate origin at the centroid of a unit cell. These are the reasons why we are using the form of the constitutive Equation (1) in this work.

To determine the effective stiffnesses $D_{\alpha\beta}$ (α, β = 1, 2, 3, 4, 5, 6) of composite Timoshenko beams, six generalized beam strain states $\boldsymbol{\varepsilon}_{1\mathrm{D}}^{[\alpha]}$ or $\boldsymbol{\varepsilon}_{1\mathrm{D}}^{[\beta]}$ were considered as:

$$\boldsymbol{\varepsilon}_{1\mathrm{D}} = \begin{bmatrix} \varepsilon_1 \\ \kappa_3 \\ \kappa_2 \\ \kappa_1 \\ \gamma_{12} \\ \gamma_{13} \end{bmatrix}, \quad \boldsymbol{\varepsilon}_{1\mathrm{D}}^{[1]} = \begin{bmatrix} 1 \\ 0 \\ 0 \\ 0 \\ 0 \\ 0 \end{bmatrix}, \quad \boldsymbol{\varepsilon}_{1\mathrm{D}}^{[2]} = \begin{bmatrix} 0 \\ 1 \\ 0 \\ 0 \\ 0 \\ 0 \end{bmatrix}, \quad \boldsymbol{\varepsilon}_{1\mathrm{D}}^{[3]} = \begin{bmatrix} 0 \\ 0 \\ 1 \\ 0 \\ 0 \\ 0 \end{bmatrix}, \quad \boldsymbol{\varepsilon}_{1\mathrm{D}}^{[4]} = \begin{bmatrix} 0 \\ 0 \\ 0 \\ 1 \\ 0 \\ 0 \end{bmatrix}, \quad \boldsymbol{\varepsilon}_{1\mathrm{D}}^{[5]} = \begin{bmatrix} 0 \\ y_1 \\ 0 \\ 0 \\ C_{12} \\ 0 \end{bmatrix}, \quad \boldsymbol{\varepsilon}_{1\mathrm{D}}^{[6]} = \begin{bmatrix} 0 \\ 0 \\ y_1 \\ 0 \\ 0 \\ C_{13} \end{bmatrix} \tag{2}$$

where C_{12} and C_{13} are constant shear strains determined by equilibrium equations of beams, and the results are $C_{12} = D_{22}/D_{55}$ and $C_{13} = D_{33}/D_{66}$. The six 3D homogenized elastic strains $\boldsymbol{\varepsilon}_{3\mathrm{D}}^{0[\alpha]}$ or $\boldsymbol{\varepsilon}_{3\mathrm{D}}^{0[\beta]}$ matching to $\boldsymbol{\varepsilon}_{1\mathrm{D}}^{[\alpha]}$ or $\boldsymbol{\varepsilon}_{1\mathrm{D}}^{[\beta]}$ are:

$$\boldsymbol{\varepsilon}_{3\mathrm{D}}^{0} = \begin{bmatrix} \varepsilon_{11}^0 \\ \varepsilon_{22}^0 \\ \varepsilon_{33}^0 \\ 2\varepsilon_{23}^0 \\ 2\varepsilon_{13}^0 \\ 2\varepsilon_{12}^0 \end{bmatrix}, \quad \boldsymbol{\varepsilon}_{3\mathrm{D}}^{0[1]} = \begin{bmatrix} 1 \\ 0 \\ 0 \\ 0 \\ 0 \\ 0 \end{bmatrix}, \quad \boldsymbol{\varepsilon}_{3\mathrm{D}}^{0[2]} = \begin{bmatrix} y_2 \\ 0 \\ 0 \\ 0 \\ 0 \\ 0 \end{bmatrix}, \quad \boldsymbol{\varepsilon}_{3\mathrm{D}}^{0[3]} = \begin{bmatrix} y_3 \\ 0 \\ 0 \\ 0 \\ 0 \\ 0 \end{bmatrix}, \quad \boldsymbol{\varepsilon}_{3\mathrm{D}}^{0[4]} = \begin{bmatrix} 0 \\ 0 \\ 0 \\ 0 \\ -y_2 \\ y_3 \end{bmatrix}, \quad \boldsymbol{\varepsilon}_{3\mathrm{D}}^{0[5]} = \begin{bmatrix} y_1 y_2 \\ 0 \\ 0 \\ 0 \\ 0 \\ C_{12} \end{bmatrix}, \quad \boldsymbol{\varepsilon}_{3\mathrm{D}}^{0[6]} = \begin{bmatrix} y_1 y_3 \\ 0 \\ 0 \\ 0 \\ C_{13} \\ 0 \end{bmatrix} \tag{3}$$

With the given homogenized strain states $\boldsymbol{\varepsilon}_{3\mathrm{D}}^{0[\alpha]}$ (or $\varepsilon_{mn}^{0[\alpha]}$), the elastic tensor E_{ijmn} (i, j, m, n = 1, 2, 3 for 3D problems), and the constraint conditions (including periodicity and normalization) in [22], one can solve the following self-equilibrium equation of a unit cell problem within the cell domain V to obtain the perturbed elastic strains $\varepsilon_{mn}^{1[\alpha]}$:

$$\begin{cases} \sigma_{ij,j}^{[\alpha]} = 0 \text{ in } V \\ \sigma_{ij}^{[\alpha]} n_j = 0 \text{ on } \mathrm{S_{np}} \\ \sigma_{ij}^{[\alpha]} = E_{ijmn} \varepsilon_{mn}^{[\alpha]} \\ \varepsilon_{mn}^{[\alpha]} = \varepsilon_{mn}^{0[\alpha]} + \varepsilon_{mn}^{1[\alpha]} \end{cases} \tag{4}$$

where S_{np} represents the non-periodic faces of a unit cell. The detailed procedure for solving Equation (4) can be found in Section 2.2 of reference [22]. Then, the six corresponding microscopic strains $\varepsilon_{mn}^{[\alpha]}$ and microscopic stresses $\sigma_{ij}^{[\alpha]}$ are obtained.

Finally, the diagonal effective stiffnesses can be calculated by:

$$D_{\alpha\alpha} = \frac{1}{l} \int_V \varepsilon_{ij}^{[\alpha]} E_{ijmn} \varepsilon_{mn}^{[\alpha]} \mathrm{d}V, \ \alpha = 1, 2, 3, 4 \tag{5}$$

$$D_{55} = \frac{l D_{22}^2}{\int_{\mathrm{V}} \varepsilon_{ij}^{[5]} E_{ijmn} \varepsilon_{mn}^{[5]} \mathrm{dV} - l^3 D_{22}/12} \tag{6}$$

$$D_{66} = \frac{l D_{33}^2}{\int_{\mathrm{V}} \varepsilon_{ij}^{[6]} E_{ijmn} \varepsilon_{mn}^{[6]} \mathrm{dV} - l^3 D_{33}/12} \tag{7}$$

And the shearing-torsion couplings $D_{\alpha 4}$ (α = 5, 6) are achieved with:

$$\begin{bmatrix} D_{54} \\ D_{64} \end{bmatrix} = \frac{1}{l} \begin{bmatrix} \int_V \sigma_{12}^{[4]} \mathrm{d}V \\ \int_V \sigma_{13}^{[4]} \mathrm{d}V \end{bmatrix} \tag{8}$$

where l denotes the cell length. For structures with other types of couplings, more strain states need to be considered to establish all the relationships between the effective stiffnesses according to the similar solution process given in Section 2 in [22]. It should also be noted that the formulae for calculating microscopic stresses in Section 3 still hold when off-diagonal terms exist.

With the attained effective stiffnesses, one can obtain the generalized solutions of the macroscopic equivalent beam. This homogenization method works well for stiffness problems (including frequency and mode shapes), but it cannot be used for stress-related strength analysis.

To predict the microscopic stresses of the original 3D heterogeneous beam structure, the above attained $\sigma_{ij}^{[\alpha]}$ of the unit cell problems serve as six basic stress solutions in the present prediction. In addition, to make the physical meanings of the basic stress solutions more clear, the last two linear curvature states in Equation (2) are replaced by two unit shear states, then their corresponding microscopic strains and stresses become:

$$\boldsymbol{\varepsilon}_{1\mathrm{D}}^{[5]*} = \begin{bmatrix} 0 & 0 & 0 & 0 & 1 & 0 \end{bmatrix}^{\mathrm{T}} \Rightarrow \begin{cases} \varepsilon_{mn}^{[5]*} = \left(\varepsilon_{mn}^{[5]} - y_1 \varepsilon_{mn}^{[2]}\right)/C_{12} \\ \sigma_{ij}^{[5]*} = \left(\sigma_{ij}^{[5]} - y_1 \sigma_{ij}^{[2]}\right)/C_{12} \end{cases} \tag{9}$$

$$\boldsymbol{\varepsilon}_{1\mathrm{D}}^{[6]*} = \begin{bmatrix} 0 & 0 & 0 & 0 & 0 & 1 \end{bmatrix}^{\mathrm{T}} \Rightarrow \begin{cases} \varepsilon_{mn}^{[6]*} = \left(\varepsilon_{mn}^{[6]} - y_1 \varepsilon_{mn}^{[3]}\right)/C_{13} \\ \sigma_{ij}^{[6]*} = \left(\sigma_{ij}^{[6]} - y_1 \sigma_{ij}^{[3]}\right)/C_{13} \end{cases} \tag{10}$$

In addition, we define $\boldsymbol{\varepsilon}_{1\mathrm{D}}^{[\alpha]*} = \boldsymbol{\varepsilon}_{1\mathrm{D}}^{[\alpha]}$, $\varepsilon_{mn}^{[\alpha]*} = \varepsilon_{mn}^{[\alpha]}$, and $\sigma_{ij}^{[\alpha]*} = \sigma_{ij}^{[\alpha]}$ for α = 1, 2, 3, 4 for later derivation clarification, and these field variables with the superscript "$[\alpha]*$" (α = 1, 2, 3, 4, 5, 6) respectively correspond to six generalized unit beam strain states. For instance, $\boldsymbol{\varepsilon}_{1\mathrm{D}}^{[5]*}$ stands for the unit shear strain state of a Timoshenko beam, while $\varepsilon_{mn}^{[5]*}$ and $\sigma_{ij}^{[5]*}$ denote the microscopic elastic strains and stresses under this unit shear strain state.

3. The Formulae for Calculating Microscopic Stresses

For predicting the microscopic stresses of a 3D heterogeneous structure with the microscopic stresses of unit cell problems, we propose a multiscale model as follows:

$$\sigma_{ij}(x_1, \boldsymbol{y}) = a_\alpha(x_1)\sigma_{ij}^{[\alpha]*}(\boldsymbol{y}) = a_1\sigma_{ij}^{[1]*} + a_2\sigma_{ij}^{[2]*} + \cdots + a_6\sigma_{ij}^{[6]*} \tag{11}$$

where x_1 is the macroscopic coordinate for equivalent beams, and $\boldsymbol{y}$ = (y_1, y_2, y_3) are the microscopic coordinates for 3D unit cells. The two-scale equivalence of the internal virtual work at a structural level is employed to determine the coefficients a_α, i.e., $\boldsymbol{a} = [a_1\ a_2\ a_3\ a_4\ a_5\ a_6]^{\mathrm{T}}$.

The internal virtual work of the macroscopic beam is $\int_L (\boldsymbol{F}^{\mathrm{T}}\delta\varepsilon_{1\mathrm{D}})\mathrm{d}x_1$, while the internal virtual work of the 3D heterogeneous structure is $\iiint_\Omega \langle \boldsymbol{\sigma}_{3\mathrm{D}}^{\mathrm{T}}\delta\boldsymbol{\varepsilon}_{3\mathrm{D}}\rangle \mathrm{d}x_1\mathrm{d}x_2\mathrm{d}x_3$. The equivalence between them gives:

$$\int_L \left(\boldsymbol{F}^{\mathrm{T}}\delta\varepsilon_{1\mathrm{D}}\right)\mathrm{d}x_1 = \iiint_\Omega \left\langle \boldsymbol{\sigma}_{3\mathrm{D}}^{\mathrm{T}}\delta\boldsymbol{\varepsilon}_{3\mathrm{D}}\right\rangle \mathrm{d}x_1\mathrm{d}x_2\mathrm{d}x_3 \tag{12}$$

where L and Ω respectively denote the structural length and the region; $\langle\cdot\rangle$ is the average operator defined over the unit cell domain V as:

$$\langle\cdot\rangle = \frac{1}{|V|}\int_V (\cdot)\mathrm{d}V = \frac{1}{|V|}\iiint_V (\cdot)\mathrm{d}y_1\mathrm{d}y_2\mathrm{d}y_3 \tag{13}$$

Let the virtual strains $\delta\boldsymbol{\varepsilon}_{1\mathrm{D}}$ and $\delta\boldsymbol{\varepsilon}_{3\mathrm{D}}$ be:

$$\begin{cases} \delta\boldsymbol{\varepsilon}_{1\mathrm{D}} = \boldsymbol{\varepsilon}_{1\mathrm{D}}^{[\beta]*} \\ \delta\boldsymbol{\varepsilon}_{3\mathrm{D}} = \boldsymbol{\varepsilon}_{3\mathrm{D}}^{[\beta]*} \end{cases} \tag{14}$$

Substituting Equation (14) into Equation (12) yields:

$$\int_L \left(\boldsymbol{F}^{\mathrm{T}} \boldsymbol{\varepsilon}_{\mathrm{1D}}^{[\beta]*} \right) \mathrm{d}x_1 = \iiint_\Omega \left\langle \boldsymbol{\sigma}_{\mathrm{3D}}^{\mathrm{T}} \boldsymbol{\varepsilon}_{\mathrm{3D}}^{[\beta]*} \right\rangle \mathrm{d}x_1 \mathrm{d}x_2 \mathrm{d}x_3 \tag{15}$$

Then, inserting Equation (11) into Equation (15) gives:

$$\int_L \left(\boldsymbol{F}^{\mathrm{T}} \boldsymbol{\varepsilon}_{\mathrm{1D}}^{[\beta]*} \right) \mathrm{d}x_1 = \iiint_\Omega a_\alpha \left\langle \boldsymbol{\sigma}_{\mathrm{3D}}^{[\alpha]*\mathrm{T}} \boldsymbol{\varepsilon}_{\mathrm{3D}}^{[\beta]*} \right\rangle \mathrm{d}x_1 \mathrm{d}x_2 \mathrm{d}x_3 \tag{16}$$

According to the internal virtual work equivalence at a unit cell level [36], one has:

$$\left\langle \boldsymbol{\sigma}_{\mathrm{3D}}^{[\alpha]*\mathrm{T}} \boldsymbol{\varepsilon}_{\mathrm{3D}}^{[\beta]*} \right\rangle = l D_{\alpha\beta} / V \tag{17}$$

Then:

$$\int_L \left(\boldsymbol{F}^{\mathrm{T}} \boldsymbol{\varepsilon}_{\mathrm{1D}}^{[\beta]*} - D_{\alpha\beta} a_\alpha \right) \mathrm{d}x_1 = 0 \tag{18}$$

To make Equation (18) hold for arbitrary real loads, we let:

$$\boldsymbol{F}^{\mathrm{T}} \boldsymbol{\varepsilon}_{\mathrm{1D}}^{[\beta]*} - D_{\alpha\beta} a_\alpha = 0 \tag{19}$$

Equation (19) holds for $\beta = 1,\ 2, \cdots, 6$, which means:

$$\begin{cases} \boldsymbol{F}^{\mathrm{T}} \boldsymbol{\varepsilon}_{\mathrm{1D}}^{[1]*} - D_{\alpha 1} a_\alpha = 0 \\ \boldsymbol{F}^{\mathrm{T}} \boldsymbol{\varepsilon}_{\mathrm{1D}}^{[2]*} - D_{\alpha 2} a_\alpha = 0 \\ \qquad \vdots \\ \boldsymbol{F}^{\mathrm{T}} \boldsymbol{\varepsilon}_{\mathrm{1D}}^{[6]*} - D_{\alpha 6} a_\alpha = 0 \end{cases} \tag{20}$$

Or:

$$\begin{bmatrix} \boldsymbol{\varepsilon}_{\mathrm{1D}}^{[1]*} & \boldsymbol{\varepsilon}_{\mathrm{1D}}^{[2]*} & \cdots & \boldsymbol{\varepsilon}_{\mathrm{1D}}^{[6]*} \end{bmatrix}^{\mathrm{T}} \boldsymbol{F} - \boldsymbol{D}\boldsymbol{a} = 0 \tag{21}$$

Because $\begin{bmatrix} \boldsymbol{\varepsilon}_{\mathrm{1D}}^{[1]*} & \boldsymbol{\varepsilon}_{\mathrm{1D}}^{[2]*} & \cdots & \boldsymbol{\varepsilon}_{\mathrm{1D}}^{[6]*} \end{bmatrix}$ is the identity matrix, Equation (21) changes to:

$$\boldsymbol{F} = \boldsymbol{D}\boldsymbol{a} \tag{22}$$

Then we can obtain:

$$\boldsymbol{a} = \boldsymbol{D}^{-1} \boldsymbol{F} = \boldsymbol{\varepsilon}_{\mathrm{1D}} \tag{23}$$

With the obtained $\boldsymbol{a}$, we can calculate the microscopic stresses with Equation (11).

4. Numerical Examples

In this section, several numerical examples are given to validate the effectiveness of the present method in predicting the microscopic stresses of composite beams. The coordinate origins of these symmetric structures are set at the center of the left ends, and "FEM" is used to denote the reference solutions obtained by the finite element software Comsol Multiphysics.

4.1. A Sandwich Beam with Square Cores

Consider a periodic sandwich beam [15], as illustrated in Figure 1. The parameters related to the unit cell are l = 1.5 m, b = 1.5 m, a = 1 m, t = 0.1 m, $2h$ = 3 m. The length of this beam is L = 60 m (40 unit cells). The material parameters for surface parts are E_1 = 70 GPa and ν_1 = 0.34, while core parts are E_2 = 3.5 GPa and ν_2 = 0.34. The unit cell is discretized by 18,400 quadratic hexahedral elements, and the whole structure has a total of 736,000 elements for direct analysis.

The left end of the beam is fixed, and the right end is free. There is a bending moment $M_2 = 1.60 \times 10^5$ N·m acting on the free end. The present microscopic stress components

σ_{11}, σ_{22}, and σ_{33} at the line $(x_1 = 30\text{ m},\ x_2 = 0)$ are compared with those of the VABS [15] and the FEM in Figures 2–4, and the comparisons show the present results have good agreement with the referenced ones, validating the accuracy of this proposed method.

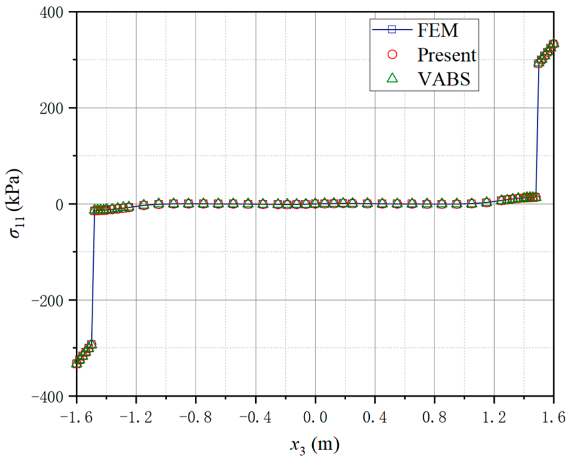

Figure 2. Distribution of σ_{11} of the sandwich beam along x_3 at $x_1 = 30\text{ m},\ x_2 = 0$.

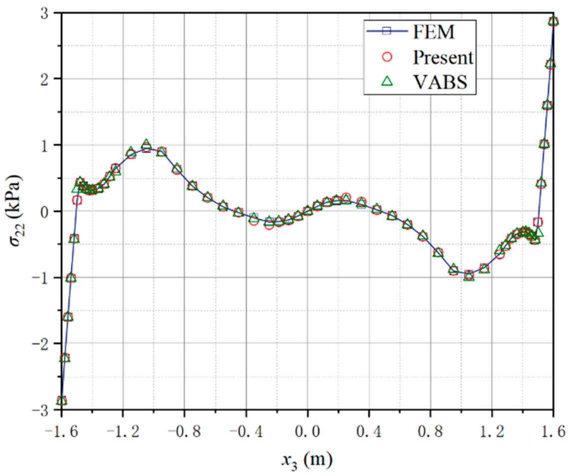

Figure 3. Distribution of σ_{22} of the sandwich beam along x_3 at $x_1 = 30\text{ m},\ x_2 = 0$.

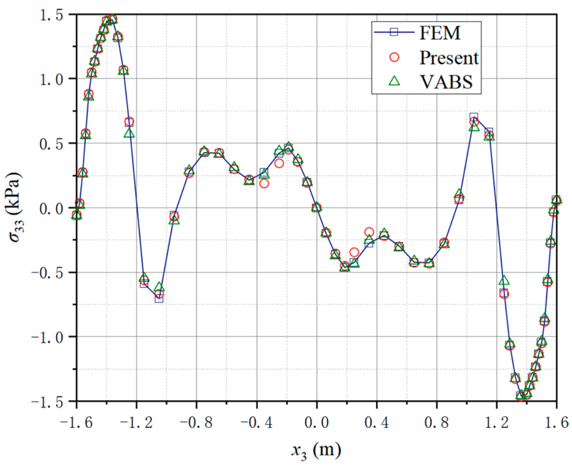

Figure 4. Distribution of σ_{33} of the sandwich beam along x_3 at $x_1 = 30\text{ m},\ x_2 = 0$.

4.2. A Three-Way Perforated Beam

In Figure 5, a three-way perforated cantilever beam is considered. The geometric parameters of one unit cell are $a = 1.2$ m, $l = b = h = 2$ m. The length of the beam with 20 unit cells is L = 40 m. The material parameters are E = 206 GPa and ν = 0.3. The unit cell is discretized by 2816 quadratic hexahedral elements, while the whole structure for obtaining reference solutions has a total of 56,320 elements.

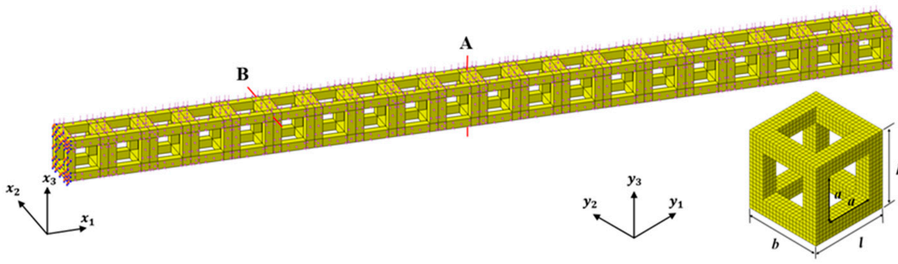

Figure 5. Three-way perforated beam and its unit cell.

Both top and front surfaces of this beam are subjected to distributed loads, as $q_3 = -1000$ Pa (along the x_3 direction) on the top and q_2 = 2000 Pa (along the x_2 direction) at the front. The stress components σ_{11}, σ_{12}, and σ_{13} of the present method and the FEM are compared. The comparison results for Line A (x_1 = 20 m, x_2 = 0.8 m) are in Figures 6–8, while those for Line B (x_1 = 10 m, x_3 = 0.8 m) are in Figures 9–11. It can be seen that the present results are in excellent agreement with the reference results.

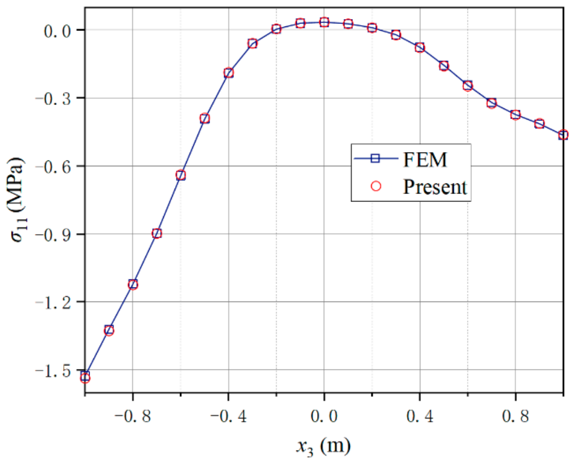

Figure 6. Distribution of σ_{11} of the three-way perforated beam at Line A.

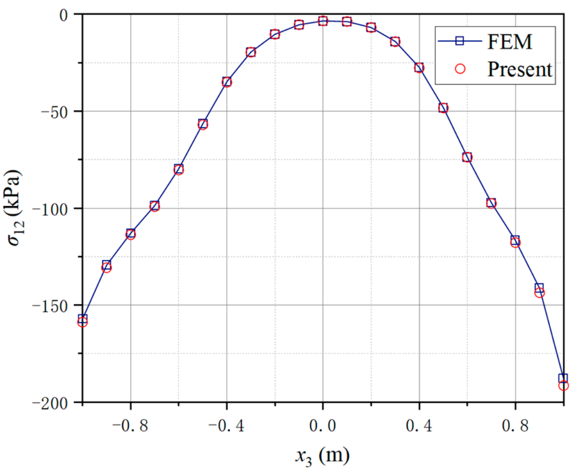

Figure 7. Distribution of σ_{12} of the three-way perforated beam at Line A.

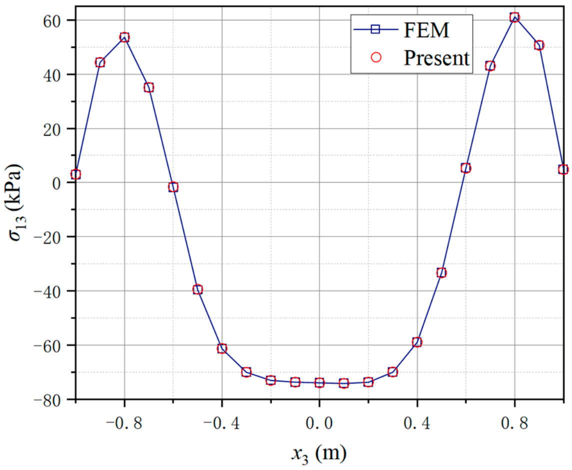

Figure 8. Distribution of σ_{13} of the three-way perforated beam at Line A.

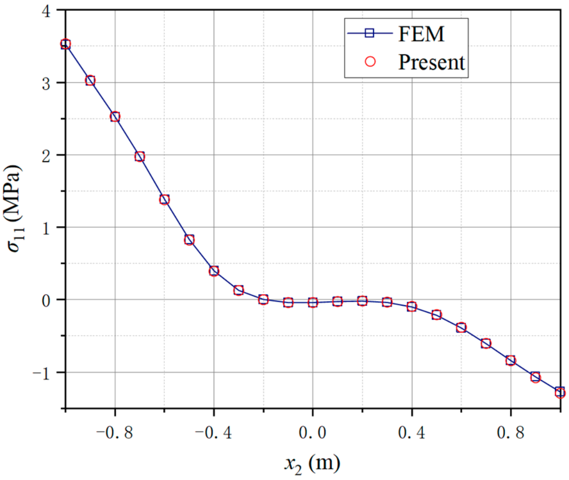

Figure 9. Distribution of σ_{11} of the three-way perforated beam at Line B.

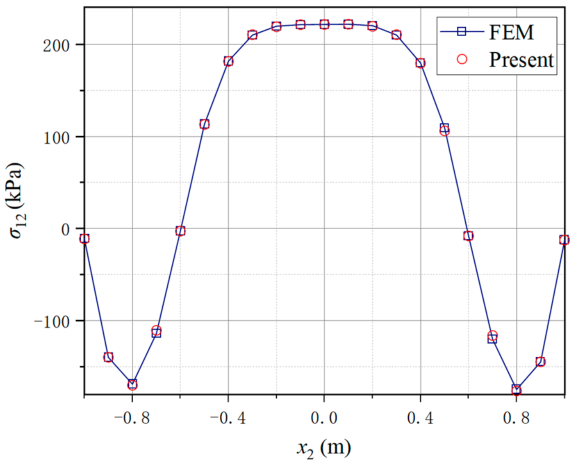

Figure 10. Distribution of σ_{12} of the three-way perforated beam at Line B.

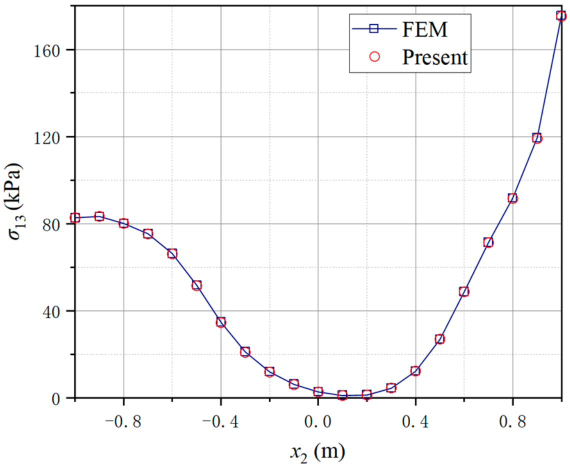

Figure 11. Distribution of σ_{13} of the three-way perforated beam at Line B.

4.3. A Honeycomb-Core Sandwich Beam

In this example, a honeycomb beam is considered in Figure 12. The geometric parameters of honeycomb [4] are $l = \sqrt{3}$ m, $b = 1$ m, $l_1 = \sqrt{3}/3$ m, $t = 1/6$ m, $h_f = 0.2$ m, $h_c = 2$ m. This beam consists of 20 unit cells. The material parameters are E_1 = 7 GPa, ν_1 = 0.34 (surface material); E_2 = 3.5 GPa, ν_2 = 0.34 (core material). The unit cell is discretized by 7328 quadratic hexahedral elements, and the whole structure has a total of 146,560 elements.

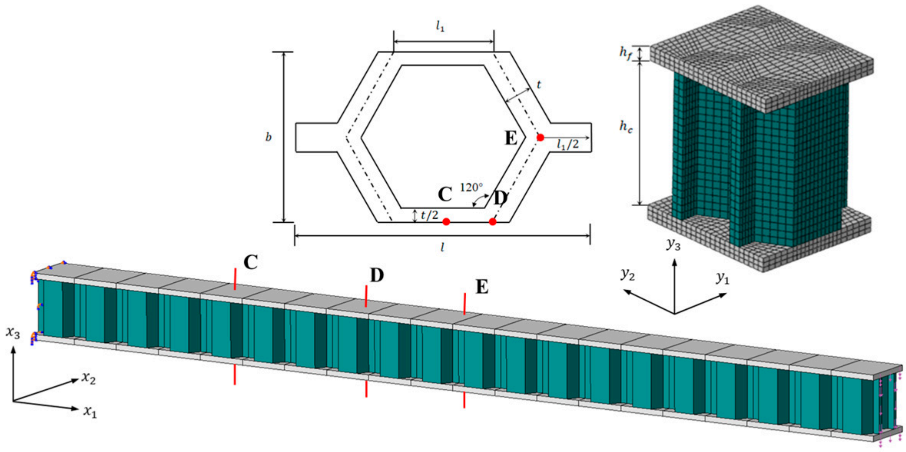

Figure 12. Honeycomb-core sandwich beam and its unit cell.

The beam, with the left end clamped, is subjected to a distributed load $q = -1000$ Pa at the free-end surface. The microscopic stresses σ_{11} and σ_{13} at Line C ($x_1 = 4.5\sqrt{3}$ m, $x_2 = 0$), Line D ($x_1 = 23\sqrt{3}/3$ m, $x_2 = 0$), and Line E ($x_1 = 59\sqrt{3}/6$ m, $x_2 = 0.5$ m) (see their positions in a unit cell in Figure 12) are calculated by the present method. These three lines are selected according to their proximity to the structure boundary, and to better show the validity and applicability of the present method. The comparison results with those of FEM are displayed in Figures 13–18. The good coincidence with the FEM validates that the present method is capable of solving the microscopic stresses of composite beams with complex microstructures.

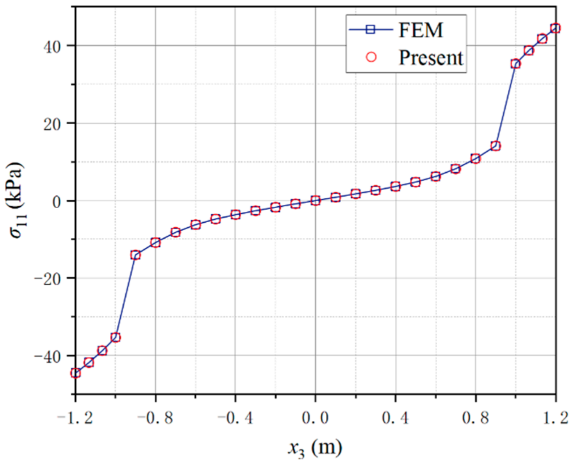

Figure 13. Distribution of σ_{11} of the honeycomb-core beam at Line C.

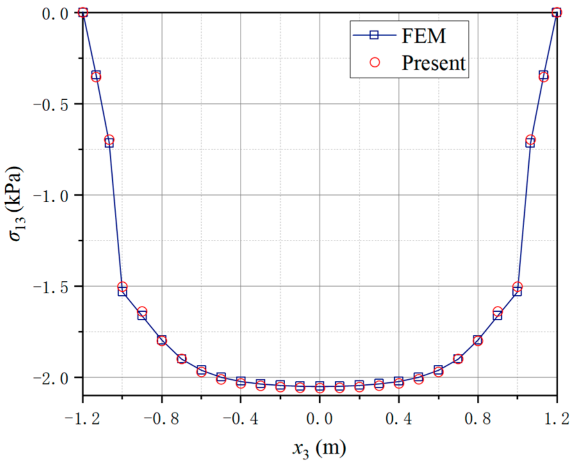

Figure 14. Distribution of σ_{13} of the honeycomb-core beam at Line C.

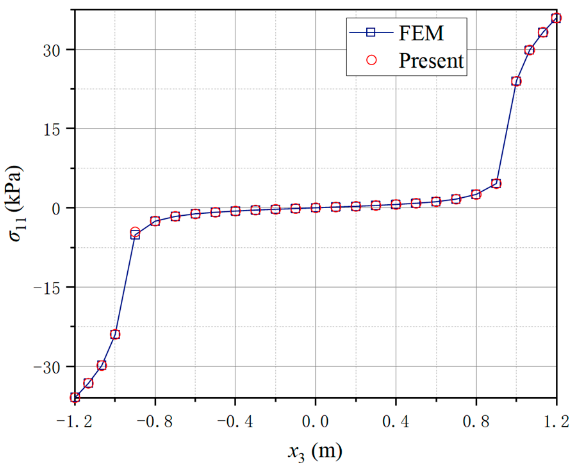

Figure 15. Distribution of σ_{11} of the honeycomb-core beam at Line D.

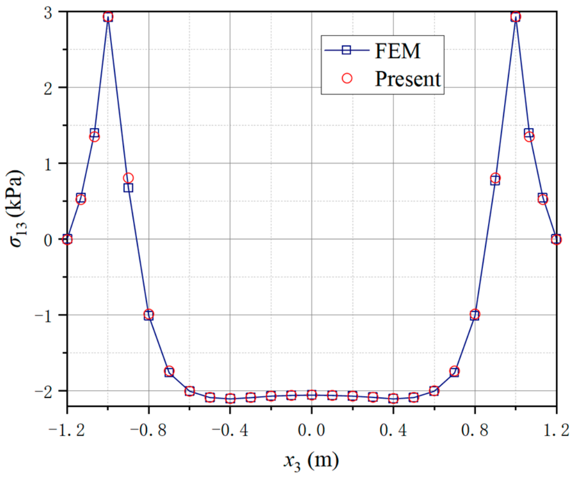

Figure 16. Distribution of σ_{13} of the honeycomb-core beam at Line D.

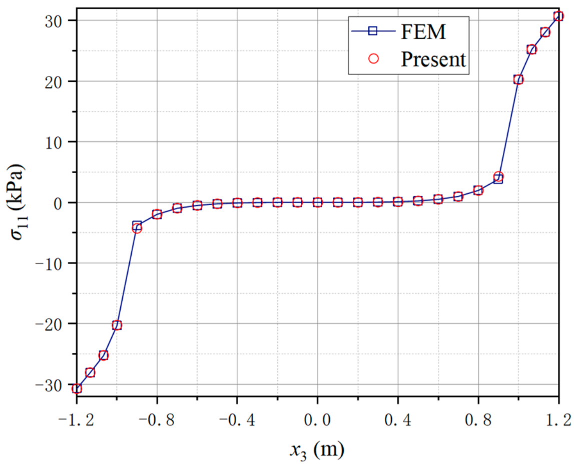

Figure 17. Distribution of σ_{11} of the honeycomb-core beam at Line E.

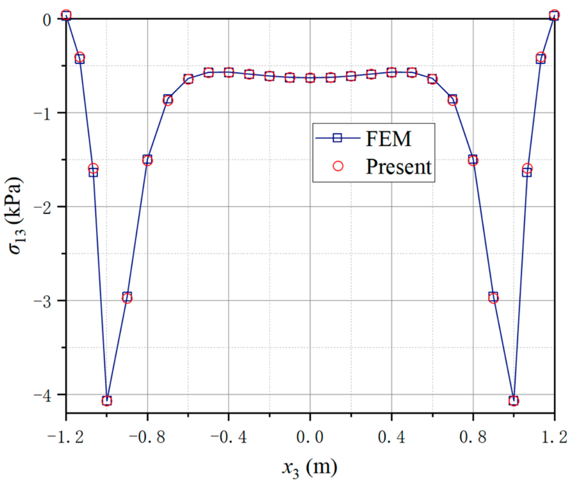

Figure 18. Distribution of σ_{13} of the honeycomb-core beam at Line E.

5. Conclusions

This work extended a recently proposed homogenization method to local or microscopic stress analysis of 3D periodic beam-like structures; to realize this homogenization to dehomogenization process, a novel superposition method was proposed. In this method, six kinds of microscopic stress solutions of the unit cell problem used for the effective stiffness prediction (or homogenization) of composite beams were transformed into corresponding microscopic stresses under six generalized unit beam strain states, and then they were regarded as basic stress solutions in the superposition. In addition, the internal work equivalence at the structural level, including the original 3D heterogeneous structure and the homogenized 1D beam structure, was employed to determine the six superposition coefficients, and they were proved to be equal to the actual generalized beam strains.

The six microscopic stress solutions of the 3D unit cell problem serving as the basis have clear physical meanings because they were generated by the six generalized unit beam strains, including one tension, two bendings, one torsion, and two shearings. This further illustrates the reasonableness of the six superposition coefficients.

The structural microscopic stresses obtained by the present method have been compared with those of the 3D finite element method, and they were fairly consistent for several examples with different microstructures and loads, demonstrating the validity and capability of the proposed method. Furthermore, this method has a superiority in efficiency because only one unit cell rather than the entire structure composed of all unit cells was employed for reaching the desired microscopic stresses.

Author Contributions: Conceptualization, Y.X., Z.H., and Y.G.; formal analysis, L.M.; funding acquisition, Y.X. and Y.G.; investigation, L.M.; software, L.M.; supervision, Y.X. and Y.G.; validation, L.M.; writing—original draft, Y.X., L.M., and Y.G.; writing—review and editing, Y.G. All authors have read and agreed to the published version of the manuscript.

Funding: This work was funded by the National Natural Science Foundation of China (grant numbers 12002019 and 12172023) and the China Postdoctoral Science Foundation (grant numbers 2021T140040).

Data Availability Statement: Not applicable.

Conflicts of Interest: The authors declare no conflict of interest.

References

1. Bensoussan, A.; Lions, J.L.; Papanicolaou, G. *Asymptotic Analysis for Periodic Structures*; Elsevier: Amsterdam, The Netherlands, 1978.
2. Oleinik, O.A.; Shamaev, A.S.; Yosifian, G.A. *Mathematical Problems in Elasticity and Homogenization*; Elsevier: Amsterdam, The Netherlands, 1992.
3. Dai, G.M.; Zhang, W.H. Size effects of basic cell in static analysis of sandwich beams. *Int. J. Solids Struct.* **2008**, *45*, 2512–2533. [CrossRef]
4. Dai, G.M.; Zhang, W.H. Cell size effects for vibration analysis and design of sandwich beams. *Acta Mech. Sin.* **2009**, *25*, 353–365. [CrossRef]
5. Yi, S.A.; Xu, L.; Cheng, G.D.; Cai, Y.W. FEM formulation of homogenization method for effective properties of periodic heterogeneous beam and size effect of basic cell in thickness direction. *Comput. Struct.* **2015**, *156*, 1–11. [CrossRef]
6. Kolpakov, A.G. Calculation of the characteristics of thin elastic rods with a periodic structure. *J. Appl. Math. Mech.* **1991**, *55*, 358–365. [CrossRef]
7. Kolpakov, A.G. Variational principles for stiffnesses of a non-homogeneous beam. *J. Mech. Phys. Solids* **1998**, *46*, 1039–1053. [CrossRef]
8. Kolpakov, A.G. *Stressed Composite Structures: Homogenized Models for Thin-Walled Nonhomogeneous Structures with Initial Stresses*; Springer: Berlin/Heidelberg, Germany; New York, USA, 2004.
9. Cesnik, C.E.S.; Hodges, D.H.; Sutyrin, V.G. Cross-sectional analysis of composite beams including large initial twist and curvature effects. *AIAA J.* **1996**, *34*, 1913–1920. [CrossRef]
10. Cesnik, C.E.S.; Sutyrin, V.G.; Hodges, D.H. Refined theory of twisted and curved composite beams: The role of short-wavelength extrapolation. *Int. J. Solids Struct.* **1996**, *33*, 1387–1408. [CrossRef]
11. Cesnik, C.E.S.; Hodges, D.H. VABS: A New Concept for Composite Rotor Blade Cross-Sectional Modeling. *J. Am. Helicopter Soc.* **1997**, *42*, 27–38. [CrossRef]
12. Popescu, B.; Hodges, D.H. On asymptotically correct Timoshenko-like anisotropic beam theory. *Int. J. Solids Struct.* **2000**, *37*, 535–558. [CrossRef]
13. Yu, W.; Hodges, D.H.; Volovoi, V.; Cesnik, C.E.S. On Timoshenko-like modeling of initially curved and twisted composite beams. *Int. J. Solids Struct.* **2002**, *39*, 5101–5121. [CrossRef]
14. Yu, W.; Hodges, D.H.; Ho, J.C. Variational asymptotic beam sectional analysis—An updated version. *Int. J. Eng. Sci.* **2012**, *59*, 40–64. [CrossRef]
15. Lee, C.Y.; Yu, W.B. Variational asymptotic modeling of composite beams with spanwise heterogeneity. *Comput. Struct.* **2011**, *89*, 1503–1511. [CrossRef]

16. Lee, C. Zeroth-Order Shear Deformation Micro-Mechanical Model for Periodic Heterogeneous Beam-like Structures. *J. Korean Soc. Power Sys. Eng.* **2015**, *19*, 55–62. [CrossRef]
17. Huang, Z.W.; Xing, Y.F.; Gao, Y.H. A two-scale asymptotic expansion method for periodic composite Euler beams. *Compos. Struct.* **2020**, *241*, 112033. [CrossRef]
18. Allaire, G. Two-scale convergence: A new method in periodic homogenization. In *Nonlinear Partial Differential Equations and Their Applications: College de France Seminar*; CRC Press: Boca Raton, FL, USA, 1994; pp. 1–14.
19. Allaire, G.g. Homogenization and Two-Scale Convergence. *SIAM J. Math. Anal.* **1992**, *23*, 1482–1518. [CrossRef]
20. Xu, L.; Cheng, G.D.; Yi, S.N. A new method of shear stiffness prediction of periodic Timoshenko beams. *Mech. Adv. Mater. Struct.* **2016**, *23*, 670–680. [CrossRef]
21. Huang, Z.W.; Xing, Y.F.; Gao, Y.H. A new method of stiffness prediction for periodic beam-like structures. *Compos. Struct.* **2021**, *267*, 113892. [CrossRef]
22. Gao, Y.H.; Huang, Z.W.; Li, G.; Xing, Y.F. A novel stiffness prediction method with constructed microscopic displacement field for periodic beam like structures. *Acta Mech. Sin.* **2022**, *38*, 421520. [CrossRef]
23. Yu, W.B.; Volovoi, V.V.; Hodges, D.H.; Hong, X.Y. Validation of the Variational Asymptotic Beam Sectional Analysis. *AIAA J.* **2002**, *40*, 2105–2112. [CrossRef]
24. Yu, W.B.; Hodges, D.H. Generalized Timoshenko theory of the variational asymptotic beam sectional analysis. *J. Am. Helicopter Soc.* **2005**, *50*, 46–55. [CrossRef]
25. Wang, Q.; Yu, W.B. Variational-asymptotic modeling of the thermoelastic behavior of composite beams. *Compos. Struct.* **2011**, *93*, 2330–2339. [CrossRef]
26. Xiao, P.; Zhong, Y.F.; Dan, L.; Bing, D. Accurate recovery of 3D local field in FRP laminated beam based on asymptotic dimension reduction model. *Constr. Build. Mater.* **2019**, *207*, 357–372. [CrossRef]
27. Liu, X.; Yu, W.B. A novel approach to analyze beam-like composite structures using mechanics of structure genome. *Adv. Eng. Softw.* **2016**, *100*, 238–251. [CrossRef]
28. Kashefi, K.; Sheikh, A.H.; Ali, M.S.M.; Griffith, M.C. An efficient modelling approach based on a rigorous cross-sectional analysis for analysing box girder bridge superstructures. *Adv. Struct. Eng.* **2016**, *19*, 513–528. [CrossRef]
29. Giavotto, V.; Borri, M.; Mantegazza, P.; Ghiringhelli, G.; Carmaschi, V.; Maffioli, G.C.; Mussi, F. Anisotropic beam theory and applications. *Comput. Struct.* **1983**, *16*, 403–413. [CrossRef]
30. Dhadwal, M.K.; Jung, S.N. Multifield Variational Sectional Analysis for Accurate Stress Computation of Multilayered Composite Beams. *AIAA J.* **2019**, *57*, 1702–1714. [CrossRef]
31. Xu, L.; Cheng, G.D. On the solutions to the Saint-Venant problem of heterogeneous beam-like structures with periodic microstructures. *Int. J. Mech. Sci.* **2019**, *163*, 105123. [CrossRef]
32. Xu, L.; Qian, Z.H. On the Almansi-Michell solution and its numerical implementation for heterogeneous beams with periodic microstructures subject to periodically-varying loads. *Compos. Struct.* **2020**, *250*, 112540. [CrossRef]
33. Treyssede, F.; Cartraud, P. A two-dimensional formulation for the homogenization of helical beam-like structures under bending loads. *Int. J. Solids Struct.* **2022**, *234*, 111270. [CrossRef]
34. Hu, Y.; Zhao, Y.; Liang, H.P. Refined Beam Theory for Geometrically Nonlinear Pre-Twisted Structures. *Aerospace* **2022**, *9*, 360. [CrossRef]
35. Sirimontree, S.; Thongchom, C.; Saffari, P.R.; Refahati, N.; Saffari, P.R. Jearsiripongkul, T.; Keawsawasvong, S. Effects of thermal environment and external mean flow on sound transmission loss of sandwich functionally graded magneto-electro-elastic cylindrical nanoshell. *Eur. J. Mech. A Solids* **2023**, *97*, 104774. [CrossRef]
36. Huang, Z.W.; Xing, Y.F.; Gao, Y.H. A new method of stiffness prediction for composite plate structures with in-plane periodicity. *Compos. Struct.* **2022**, *280*, 114850. [CrossRef]